Zeptomole-Sensitivity Electrospray Ionization-Fourier Transform Ion Cyclotron Resonance Mass Spectrometry of Proteins

ARTICLE *in* ANALYTICAL CHEMISTRY · JUNE 2000

Impact Factor: 5.64 · DOI: 10.1021/ac991360b · Source: PubMed

5 AUTHORS, INCLUDING:

Mikhail E Belov
Thermo Fisher Scientific
17 PUBLICATIONS **892** CITATIONS
SEE PROFILE

Mikhail V Gorshkov
Russian Academy of Sciences
77 PUBLICATIONS **1,238** CITATIONS
SEE PROFILE

Richard D Smith
Pacific Northwest National Laboratory
1,131 PUBLICATIONS **45,995** CITATIONS
SEE PROFILE

Anal. Chem. **2000,** *72,* 2271−2279

Zeptomole-Sensitivity Electrospray Ionization−Fourier Transform Ion Cyclotron Resonance Mass Spectrometry of Proteins

Mikhail E. Belov, Mikhail V. Gorshkov,† Harold R. Udseth, Gordon A. Anderson, and Richard D. Smith*

Environmental Molecular Sciences Laboratory, Pacific Northwest National Laboratory, P.O. Box 999, Richland, Washington 99352

Methods are being developed for ultrasensitive protein characterization based upon electrospray ionization (ESI) with Fourier transform ion cyclotron resonance mass spectrometry (FTICR-MS). The sensitivity of a FTICR mass spectrometer equipped with an ESI source depends on the overall ion transmission, which combines the probability of ionization, transmission efficiency, and ion trapping in the FTICR cell. Our developments implemented in a 3.5 tesla FTICR mass spectrometer include introduction and optimization of a newly designed electrodynamic ion funnel in the ESI interface, improving the ion beam characteristics in a quadrupole-electrostatic ion guide interface, and modification of the electrostatic ion guide. These developments provide a detection limit of approximately 30 zmol (∼18 000 molecules) for proteins with molecular weights ranging from 8 to 20 kDa.

Electrospray ionization mass spectrometry (ESI-MS) has become widely used for the study of biopolymers.[1−3] Sensitivity is often a major issue for many biological applications of ESI-MS (e.g., in proteomics, protein analysis from a single cell, and sample-limited applications in general). Fourier transform ion cyclotron resonance mass spectrometry (FTICR-MS) in conjunction with electrospray ionization provides powerful analytical capabilities for ultrasensitive protein characterization.[4−6] Improvements to the design of ESI sources have given rise to detection limits in the femtomole to attomole range.[7−9] Further increases in the sensitivity of FTICR mass spectrometers depend significantly upon increasing the overall ion transmission from solution to the FTICR cell as well as the efficiency of trapping the ions in the cell. While electrospray ionization at atmospheric pressure can be very efficient for dilute samples flowing delivered to the electrospray emitter at low flow rates, the reduction or elimination of losses during ion transport from the atmospheric pressure region of the ESI source to the second vacuum stage at a pressure of few hundred milliTorr, where transmission becomes more efficient, has been a challenge.

The recently developed "electrodynamic ion funnel" has demonstrated a substantial improvement in the ion transport efficiency through the first vacuum stage (1−5 Torr) of a mass spectrometer.[10−12] An rf field applied to the funnel electrodes creates an effective potential which confines the ion beam radially in the presence of a buffer gas, while a dc axial gradient moves the ions toward the exit electrode. The ion funnel focuses ions entering from atmospheric pressure more efficiently through a conductance-limiting orifice. This results in an effective matching to the acceptance area of a rf-only multipole ion guide, thus minimizing ion losses during ion transfer to the next lower-pressure region of the spectrometer.

In this work we report on the performance of a 3.5 tesla (T) FTICR mass spectrometer equipped with an ESI source and demonstrate high-sensitivity performance for proteins and peptides. The ESI source incorporates a newly designed ion funnel whose initial performance has recently been described.[14] Compared with the previously reported ion funnel design,[10−12] the new ion funnel has improved significantly the transmission for the total ion current, broadened m/z transmission range, and reduced collisional activation in the interface. These improvements have enabled detection limits in low zeptomolar range.

† Permanent address: Institute of Energy Problems of Chemical Physics, Russian Academy of Sciences, Moscow, Russia 117829

* To whom correspondence should be addressed

(1) Yamashita, M.; Fenn, J. B. *J. Phys. Chem.* **1984**, *88*, 4451.
(2) Fenn, J. B.; Mann, M.; Meng, C. K.; Wong, S. F.; Whitehouse, C. M. *Science (Washington, D.C.)* **1989**, *246*, 64−71.
(3) Smith, R. D.; Loo, J. A.; Edmonds, C. G. *Anal. Chem.* **1991**, *63*, 2488.
(4) Valaskovic, G. A.; Kelleher, N. L.; Little, D. P.; Aaserud, D. J.; McLaferty, F. W. *Anal. Chem.* **1995**, *67*, 3802−3805.
(5) Hofstadler, S. A.; Severs, J. C.; Smith, R. D.; Swanek, P. D.; Ewing, A. G. *Rapid Commun. Mass Spectrom.* **1996**, *10*, 919−922.
(6) Emmett, M. R.; White, F. M.; Hendrickson, C. L.; Shi, S. D.; Marshall, A. G. *J. Am. Soc. Mass Spectrom.* **1998**, *9*, 333−340.
(7) Wahl, J. H.; Goodlet, D. R.; Udseth, H. R.; Smith, R. D. *Anal. Chem.* **1992**, *64*, 3194−3196.
(8) Andren, P. E.; Emmett, M. R.; Caprioli, R. M. *J. Am. Soc. Mass Spectrom.* **1994**, *5*, 867−869.
(9) Valaskovic, G. A.; Kelleher, N. L.; McLafferty, F. W. *Science (Washington, D.C.)* **1996**, *273*, 1199−1201.
(10) Shaffer, S. A.; Tang, K.; Anderson, G. A.; Udseth, H. R.; Smith, R. D. *Rapid Commun. Mass Spectrom.* **1997**, *11*, 1813−1817.
(11) Shaffer, S. A.; Prior, D. C.; Anderson, G. A.; Udseth, H. R.; Smith, R. D. *Anal. Chem.* **1998**, *70*, 4111−4119.
(12) Shaffer, S. A.; Tolmachev, A. V.; Prior, D. C.; Anderson, G. A.; Udseth, H. R.; Smith, R. D. *Anal. Chem.* **1999**, *71*, 2957−2964.
(13) Dodonov, A.; Kozlovsky, V.; Loboda, A.; Raznikov, V.; Sulimenkov, I.; Tolmachev, A.; Kraft, A.; Wollnik, H. *Rapid Commun. Mass Spectrom.* **1997**, *11*, 1649−1656.
(14) Belov, M. E.; Gorshkov, M. V.; Udseth, H. R.; Anderson, G. A.; Tolmachev, A. V.; Prior, D. C.; Harkewicz, R.; Smith, R. D. *J. Am. Soc. Mass Spectrom.* **2000**, *11*, 19−23.

10.1021/ac991360b CCC: $19.00
Published on Web 04/12/2000

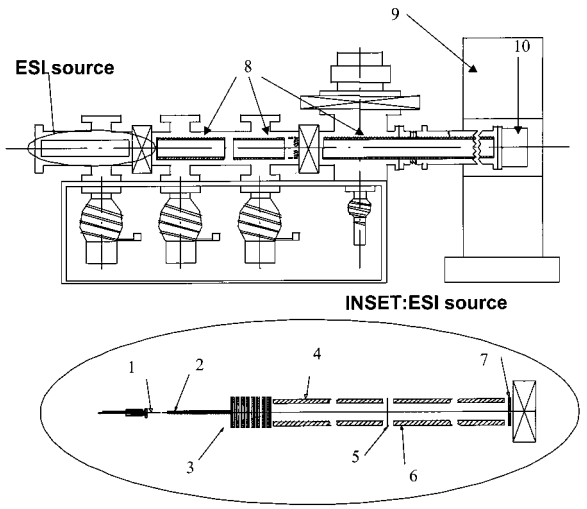

Figure 1. Schematic diagram of the 3.5 T FTICR mass spectrometer with the ESI source−ion funnel interface. 1 is the ESI emitter, 2 is the heated capillary, 3 is the ion funnel, 4 is the collisional quadrupole, 5 is the conductance limit between quadrupoles, 6 is the ion-guiding quadrupole, 7 is the exit plate of the ion-guiding quadrupole, 8 is the electrostatic ion guide, 9 is the 3.5 T superconducting magnet, 10 is the FTICR cell.

EXPERIMENTAL SECTION

A schematic illustration of the FTICR mass spectrometer developed at our laboratory, for use with both 3.5 and 11.5 T superconducting magnets,[15] is shown in Figure 1. The 3.5 T unshielded superconducting solenoid magnet (Oxford Instruments, UK) used in this work has a 33-cm diameter, horizontal room temperature bore. The mass spectrometer includes an ion funnel interface, two rf-only quadrupoles, an electrostatic ion guide, and dual cylindrical traps. Each trap is 8 cm in diameter and length. The vacuum system incorporates six stages of differential pumping which gradually decrease the pressure from atmospheric to ultrahigh vacuum in the region of the FTICR trap. The spectrometer utilizes a commercial data station and auxiliary electronics to control operation of the source and the ion guide. The ESI source and interface arrangement consists of two differentially pumped stages.

ESI emitter voltages of ∼2 kV were applied to produce positive ions. The 0.75-mm-i.d., resistively heated stainless steel inlet capillary used for droplet desolvation was maintained at ∼120 °C and typically biased at +200 to +300 V. The electrodynamic ion funnel consists of 100 electrodes of 0.5-mm thickness with the first 55 electrodes having an aperture of 25.4-mm i.d., while the apertures of the following 45 electrodes decrease linearly to 2.5-mm i.d. at the exit. The total length of the ion funnel is 100 mm. The rf voltage was applied to the funnel electrodes and was decoupled from a dc voltage power supply (Spectrum Solutions, Pittsburgh, PA) through a RC circuit. The axial gradient of a dc voltage through the funnel was from ∼300 V at the entrance electrode to ∼50 V at the exit electrode. The first stage, which incorporates the funnel, was evacuated by a 43 L/s roots pump (Leybold AG, Cologne, Germany) to ∼1 to 3 Torr. The ions transmitted through the exit electrode to the next stage are collisionally focused by a 150-mm-long quadrupole ion guide (9.525-mm rod diameter) operated in rf-only mode (typically 250 V_{p-p} at 430 kHz) at a pressure of 0.23 Torr (obtained using a 18-L/s mechanical pump, Leybold AG, Cologne, Germany) and referred to as the "collisional quadrupole" below. Direct current offset potentials of +30 to +40 V were typically applied to the quadrupole rods to assist transmission of the ions through the conductance limit between the quadrupoles. The conductance limit was biased at +10 to +15 V. The second quadrupole ion guide transmits the ions through the third pumping stage maintained at a pressure of $\sim 5 \times 10^{-5}$ Torr. In most experiments both quadrupoles were driven by the same rf power supply. However, we found that due to different pressure conditions in the quadrupoles it is advantageous to drive the quadrupoles separately to enhance the ion transmission to the electrostatic ion guide. The electrostatic ion guide in the high vacuum region of the mass spectrometer has previously been described.[15] A pressure of 8×10^{-10} to 2×10^{-9} Torr was maintained in the FTICR ion trap region.

The proteins were dissolved in a water/methanol/acetic acid solution (49:49:2 v%) at different concentrations ranging from 0.1 mg/mL to 5 ng/mL (the lowest concentration was 0.4 nM for horse cytochrome *c*). The solutions were infused into the ESI source at the flow rates of 50−200 nL/min using a syringe pump (Harvard, South Natick, MA).

RESULTS AND DISCUSSION

Compared to a multipole ion guide (e.g., a segmented quadrupole[13]) which has a limited ion acceptance for diffused ion beams or to a skimmer, the much larger effective aperture of the ion funnel makes it both more efficient and compatible with a larger-diameter heated inlet capillary used for droplet desolvation. Ion losses due to diffusion to the inlet capillary walls decrease on increasing the capillary diameter. Placing the capillary outlet at the front of a 100-mm-long funnel decreases the gas load on a multipole ion guide positioned downstream of the funnel as compared to the gas flow through a skimmer located within the Mach disk off the capillary outlet. As a result, under the same pressure conditions the aperture of the exit electrode of the funnel can be made larger than the skimmer orifice while also having a higher overall efficiency.

The charge capacity of a rf-field focusing device is based on the effective potential, which is generated by the rf-electric field. The effective potential of an ion funnel is $V^*_{funnel} \sim 1/\delta^2$, where δ is the spacing between the adjacent electrodes of the funnel (typically much less than the funnel elements's inscribed radius). The effective potential for a quadrupole is $V^*_{quad} \sim 1/r_0^2$, where r_0 is the quadrupole inscribed radius. Therefore, when the ion funnel regions and quadrupoles having the same inscribed radius are compared, the effective potential for the ion funnel is considerably higher than that of the quadrupole, provided the same rf potential is applied to both funnel and quadrupole.

Though raising the rf amplitude can increase the charge capacity of the quadrupole, the maximum rf potential in the pressure region around 1 Torr is limited by corona discharge onset. The effective potential of a quadrupole, V^*_{quad}, can be

(15) Gorshkov, M. V.; Pasa Tolic, L.; Udseth, H. R.; Anderson, G. A.; Huang, B. M.; Bruce, J. E.; Prior, D. C.; Hofstadler, S. A.; Tang, L.; Chen, L.-Z.; Willett, J. A.; Rockwood, A. L.; Sherman, M. S.; Smith, R. D. *J. Am. Soc. Mass Spectrom.* **1998**, *9*, 692−700.

determined as[16]

$$V^*_{\text{quad}} = \frac{qV_{\text{rf}}^2}{4m\omega_0^2 r_0^2} \quad (1)$$

where V_{rf} is the rf-field amplitude, m is the ion mass, q is the ion charge, ω_0 is the angular frequency of the rf-field. At $V_{\text{rf}} = 250$ V, $q = 15$, $m = 17\,000$ Da, $\omega_0 = 500$ kHz, and $r_0 = 4$ mm, $V^*_{\text{quad}} = 8$ V. V_{rf} and r_0 are based on the onset of corona discharge in the pressure region of 1 Torr and the radial size of the ion cloud exiting the heated capillary and radially expanded in a supersonic jet of air, respectively. The same effective potential can be generated by the ion funnel at V_{rf} of only 30 V. Therefore, ion capture efficiency of the ion funnel is superior to that of a segmented quadrupole, for example, which results in higher transmitted ion currents and resultant sensitivity.

The ions exiting the funnel are collisionally focused and guided through the regions of sequentially lower pressure by rf-multipole ion guides. When coupled to an electrostatic ion guide operating in high vacuum ($10^{-7} - 10^{-10}$ Torr), the operating parameters of the final multipole rf device where ions experience their last collisions with background gas, are critical for higher ion transmission and higher FTICR signal-to-noise ratio. Such parameters of a multipole as rf frequency and amplitude, pressure, axial dc-field gradient, etc. determine the emittance of the ion beam and the translational and internal energy of the ions. Choosing an appropriate operation mode for the final multipole both minimizes the translational energy spread of the ions, thus resulting in higher trapping efficiency at the same total ion current in the cell, and improves the ion transmission through the electrostatic ion guide.

The number of moles of analyte in solution injected into a FTICR mass spectrometer with an electrospray source during the time interval, t, can be formally expressed as:

$$M_{\text{inject}}[mol] = C[\text{mol/L}]Flow\_rate[\text{L/s}]t[\text{s}] \quad (2)$$

where C is the analyte concentration in mol/L, *Flow_rate* is the flow rate in L/s.

This sample consumption relates to the number of elementary charges trapped in the FTICR cell, N_{trapped}, as

$$N_{\text{trapped}} = M_{\text{inject}} q N_A T p_{\text{trap}} \quad (3)$$

where q is the average charge of an analyte ion, N_A is Avogadro's number, T is the overall transmission of analyte ions through the instrument (which includes the probability of ionization and the transmission itself), and P_{trap} is the probability of trapping the ions. The detection limit of a FTICR mass spectrometer based on sample consumption, DL[mol], corresponds to the number of elementary charges trapped in the FTICR cell producing a signal-to-noise ratio of 2.[17] For a broadband detector, this number is typically estimated to be ~100. Therefore, the detection limit can be evaluated as:

$$DL[\text{mol}] \cong \frac{100M_{\text{inject}}}{N_{\text{trapped}}} = \frac{100}{qN_A T P_{\text{trap}}} \quad (4)$$

The detection limit depends then on the overall transmission, the probability of trapping the ions in the FTICR cell, and the average number of charges, q, on the molecular ions. Therefore, higher sensitivity might be expected to be achievable in analysis of multiply protonated proteins. However, the signal for proteins is typically divided between multiple charge states as well as different isotopic peaks. As a result, actual sensitivity typically declines at high molecular weights.[17]

The present improvements in ion transmission also result from an improved coupling of the rf-only quadrupole ion guide to the electrostatic ion guide as well as on optimization of the electrostatic ion guide and the ion funnel.

Mass spectra of cytochrome *c* at two different trapping potentials obtained with a pressure of 1.6×10^{-4} Torr in the region of the rf-only quadrupole ion guide are shown in Figure 2 A. The mass spectra reveal a bimodal charge state distribution, and the ratio of intensities for $[M + 9H]^{9+}$ and $[M + 13H]^{13+}$ charge states, the most pronounced peaks of each distribution, increases with the trapping potential. The ratio of the above peak intensities as a function of the trapping potential is presented in Figure 2B. To overcome the "magnetic mirror effect",[19] the ions exiting the quadrupole are accelerated through a potential drop of about 160 V prior to entering the electrostatic ion guide by biasing the entry lens of the electrostatic ion guide to −150 V as compared with +10 V applied to the quadrupole exit lens. If one assumes a collision-free 40-mm-long acceleration region, the dependence shown in Figure 2B would be surprising, as one would expect no changes in the ratio of peak intensities upon increasing the trapping potentials. If there are ion−molecule collisions in the region of acceleration, however, "charge stripping" may become significant for higher charge states due to their larger cross sections arising from their Coulombically extended structures. Since these ion−molecule interactions would take place in the region of a strong electric field, the ions with lower number of charges formed by charge reduction from their highly protonated parents would have greater kinetic energies higher than "unstripped" molecular ions of the same charge. As a result, higher trapping potentials would be needed to decelerate the former ions as compared with that required to trap the latter. To evaluate the contribution of charge stripping in the region of acceleration, the diameter of the conductance limit between the quadrupoles was varied. Decreasing the conductance limit aperture caused a decrease in the total ion current as well as a decreased pressure in the region of the rf-only quadrupole ion guide.

The radial distribution of ions in a collisional quadrupole at ion currents ranging from 300 to about 1000 pA can be described

(16) Gerlich, D. In *State Selected and State-to-State Ion−Molecule Reaction Dynamics. Part 1. Experiment*; Ng, C. Y., Baer, M., Eds.; Advances in Chemical Physics Series, Vol. LXXXII.; Wiley: New York, 1992; pp 1−176.

(17) IUPAC Recommendations 1991 for Nomenclature and Symbolism for Mass Spectrometry; IUPAC: Research Triangle Park, NC, 1991.

(18) Smith, R. D.; Bruce, J. E.; Wu, Q.; Cheng, X.; Hofstadler, S. A.; Anderson, G. A.; Chen, R.; Bakhtiar, S. O.; Van Orden, S. O.; Gale, D. C.; Sherman, M. G.; Rockwood, A. L.; Udseth, H. R. *Mass Spectrometry in the Biological Sciences*; Burlingame, A., Carr, S., Eds.; Humana Press: Totowa, NJ, 1996; 25−68.

(19) McIver, R. T. *Int. J. Mass Spectrom. Ion Processes* **1990**, *98*, 35−50.

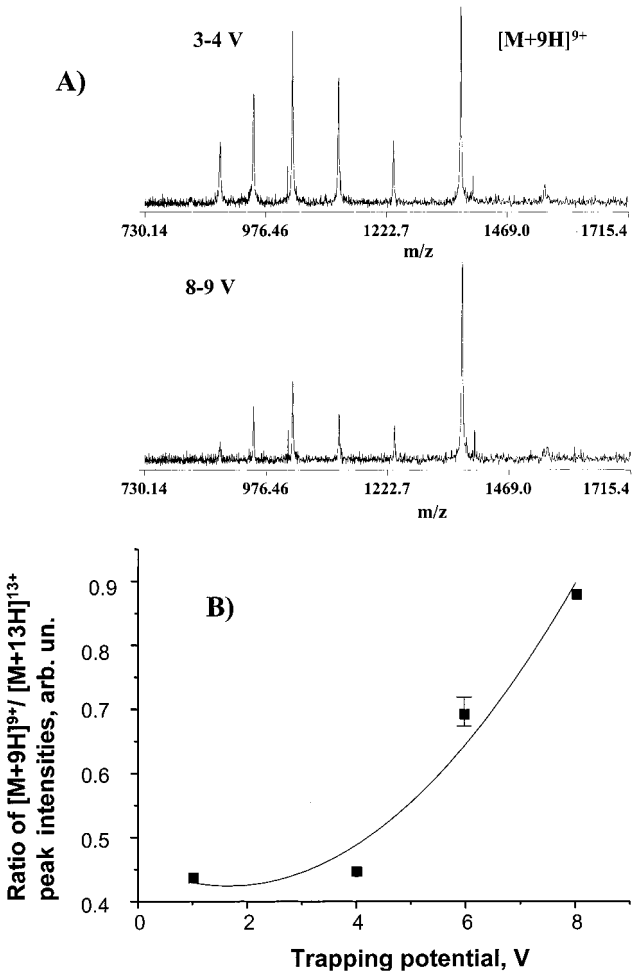

Figure 2. (A) Mass spectra of cytochrome *c* at two different trapping potentials of 3−4 V and 8−9 V, respectively. Pressure in the region of the ion-guiding quadrupole is 1.6×10^{-4} Torr. Sample concentration is 4×10^{-6} M. (B) Ratio of $[M + 9H]^{9+}$ to $[M + 12H]^{12+}$ peak intensities as a function of the trapping potential. Pressure in the ion-guiding quadrupole and sample concentration are the same as in Figure 2A.

by a Gaussian function

$$f(r) = \frac{C_0}{\sqrt{2\pi}\sigma}\exp\left(-\frac{r^2}{2\sigma^2}\right) \tag{5}$$

where C_0 and σ are the constants of Gaussian distribution and r is the radius in the polar coordinate system.

Having assumed a uniform ion distribution along the z axis, the number of ions per unit of quadrupole length sampled by the conductance limit of radius r_0 is given by

$$\frac{dN(r_0)}{dz} = 2\int_0^{\pi/2}\int_0^{r_0} f(r)r\,dr\,d\varphi \tag{6}$$

where φ is the polar angle and z is the coordinate along the quadrupole axis. Integration of eq 6 gives

$$\frac{dN(r_0)}{dz} = C_0\sqrt{\frac{\pi}{2}}\sigma^{3/2}\left[1 - \exp\left(-\frac{{r_0}^2}{2\sigma^2}\right)\right] \tag{7}$$

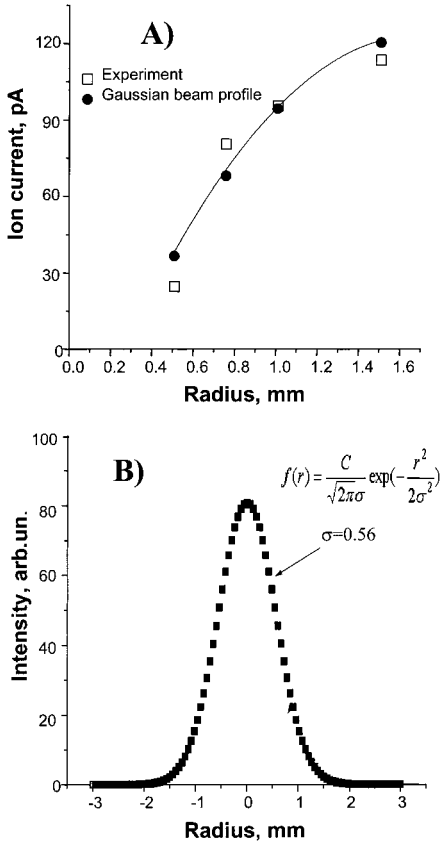

Figure 3. (A) The total ion current of cytochrome *c* at a concentration of 4×10^{-6} M in the FTICR cell as a function of the conductance limit radius. The solid line represents the best fit of a $dN(r_0)/dz$ function given by eq 7 to the experimental data points. (B) The deconvoluted radial distribution of the ion beam of cytochrome *c* in the region of the collisional-focusing quadrupole.

The total ion current transmitted to the ICR cell as a function of the conductance limit radius is presented in Figure 3A. A least-squares analysis was conducted in which $dN(r_0)/dz$ was fit to the experimental data points by varying C and σ in eq 7 (the line represents the best fit). By taking the best-fit parameters and substituting them into eq 5, the deconvoluted radial distribution of the ion beam in the collisional quadrupole was calculated and is shown in Figure 3B. As the conductance limit diameter was reduced from 3 to 2 mm, pressure in the rf-only ion guiding quadrupole decreased to about 3×10^{-5} Torr. At the same time, Figure 3B indicates that about 90% of the ion current was transmitted through the conductance limit. It is worth noting that the radial distribution of the ion beam in a quadrupole depends on the total ion current, rf amplitude, and frequency. Since both collisional and ion-guiding quadrupoles were driven by the same narrow-band high-Q head, ion transmission was optimized at a frequency of 430 kHz. The total ion current in the region of the collisional quadrupole (generally about 400 pA unless more concentrated solutions were electrosprayed) was low enough to justify the Gaussian approximation. Nevertheless, the deconvoluted radial distribution of the ion beam in the collisional quadrupole provides a useful reference for further instrumental optimization and guided the present choice of conductance limit size between the quadrupoles.

Mass spectra of cytochrome *c* and bradykinin at different pressures in the rf-only ion-guiding quadrupole are shown in

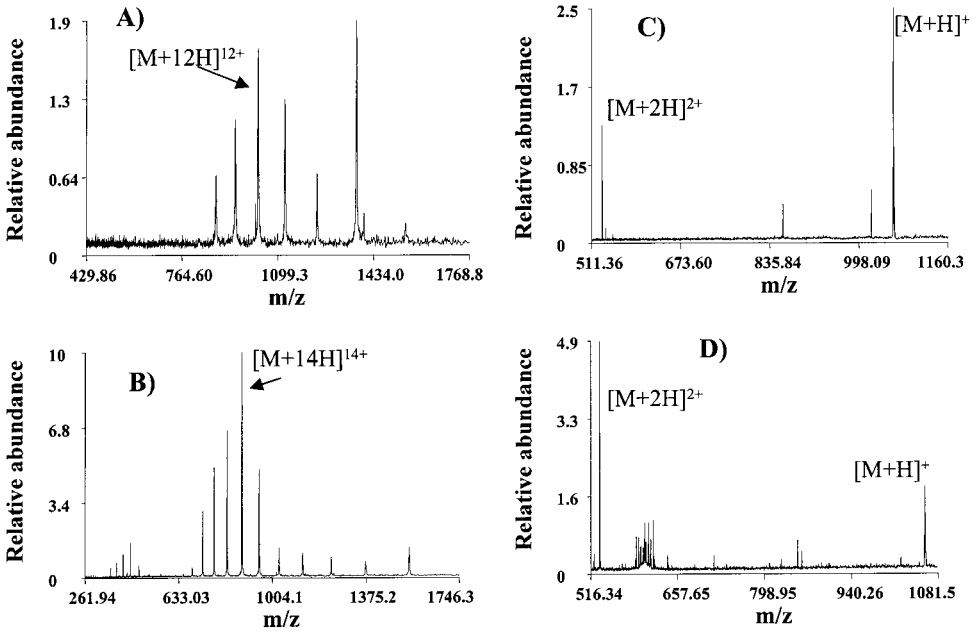

Figure 4. Mass spectra of cytochrome *c* (A,B) and bradykinin (C,D) at concentrations of 4×10^{-6} and 3×10^{-5} M, respectively. Pressure in the ion-guide quadrupole regions was 1.6×10^{-4} (A,C) and 3×10^{-5} Torr (B,D).

Figure 4. A large increase in the signal-to-noise ratio and a shift toward higher charge states are observed upon decreasing the pressure. Higher signal-to-noise ratio at lower pressure results from a narrower translational energy spread, that was measured to be about 3 eV at 3×10^{-5} Torr compared with about 8 eV at 1.6×10^{-4} Torr. Additionally, the bimodal charge state distribution of cytochrome *c* is replaced by a single mode. Further decreases in the conductance limit diameter did not reduce the translational energy spread, but resulted in lower signal-to-noise ratio due to a reduction of the ion-beam intensity. Therefore, a 2-mm-i.d. conductance limit was used in all subsequent experiments.

On the basis of SIMION 6.0[20] simulations, the electrostatic ion guide was optimized, and the instrument was then aligned with the use of a He−Ne laser. As a result, the transmission through the ion guide was improved by a factor of 7 to be in the range of 30−50%. When a conventional ESI inlet-skimmer was used for sampling the analyte ions, the total ion current detected on the rear trapping plate of the FTICR cell increased to 150 pA for 10^{-4}–10^{-6} M solutions of horse cytochrome *c*, horse myoglobin, and bovine carbonic anhydrase.

A further significant gain in analyte ion transmission was achieved by replacing the skimmer with an electrodynamic ion funnel. Preliminary results on performance of the ion funnel as a function of the ESI capillary inlet current have been reported earlier.[14] In this work the ion funnel performance was investigated as a function of the ion current entering the funnel. The inlet current was varied by moving the ESI emitter relative to the heated capillary inlet. The transmission was measured as a ratio of the ion current passed through the funnel to the total ion current introduced from the ESI inlet capillary. Similarly, ion transmission efficiency of the collisional and ion-guide quadrupole elements was also determined as a ratio of the ion current measured on the ion-guiding device positioned downstream of a particular quadrupole to the ion current measured at the quadrupole rods. Typically, ion currents of up to 4 nA and up to 2 nA were measured to the rods of the collisional and ion guiding quadrupoles, respectively, when a total ion current of 5−6 nA was introduced through the heated inlet capillary. Transmissions of the ion funnel and the collisional quadrupole as functions of the entry ion current are shown in Figure 5. The transmission of the ion funnel is virtually independent of the entry current within the range of ion currents examined. The quadrupole transmission decreases from 80% down to about 50% as the entry ion current increases to 4 nA.

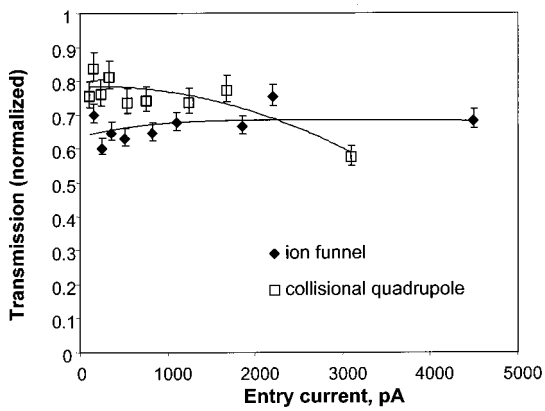

Figure 5. Transmission of the ion funnel and the collisional quadrupole as functions of the entry ion current.

The initial ion population at the exit of the heated capillary will contain many species in addition to the analyte species in the m/z range of interest. The first section of the ion funnel of constant i.d. provides an extended period for ion desolvation. This generally improves the quality of the spectra and maximizes analyte signal. However, even after complete desolvation, many charged species will still be outside the m/z range of interest (e.g., solvent ions or high m/z charged residue). These unwanted species will be

(20) Dahl D. A. *SIMION 3D*, version 6.0 User's Manual; Lockhead Idaho Technologies Co.: Idaho Falls, ID, 1995.

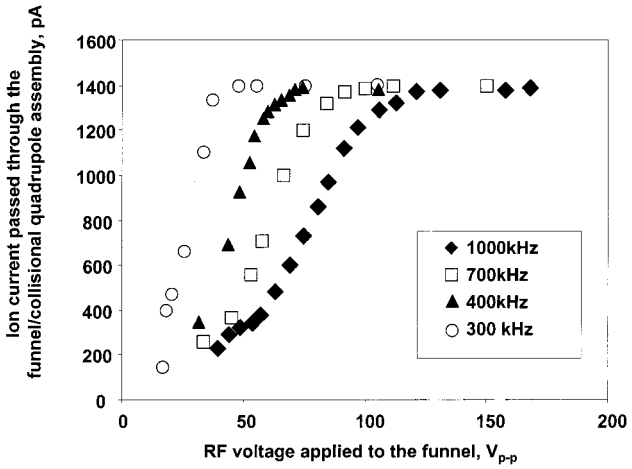

Figure 6. The output ion current of the collisional quadrupole as a function of the peak-to-peak amplitude of the rf potential applied to the ion funnel electrodes (at rf frequencies of 300 kHz, 400 kHz, 700 kHz, and 1 MHz).

efficiently rejected by the first stage rf device (the ion funnel in this work). Since one would like to operate subsequent rf quadrupoles near their space charge limit in transporting analyte ions, the first rf stage should have a charge capacity larger than a rf quadrupole, as provided by the present ion funnel design.

The output ion currents of the collisional quadrupole for different amplitudes of the rf potential applied to the funnel electrodes are shown in Figure 6. The ion current was monitored on the rods of the rf-only quadrupole ion guide since the coupling of the ion funnel to the collisional quadrupole was found to be critical for effective ion capture by the collisional quadrupole. This is attributed to ions exiting the funnel having significant radial velocities due to limited radial focusing by the funnel rf field. Thus, the collisional quadrupole should be placed as close as possible to the exit funnel plate. Maximum transmission efficiency was achieved when the collisional quadrupole was operated at a frequency of 430 kHz and at an amplitude of about 250 V_{p-p}. The ion current reaches saturation at higher rf amplitudes, corresponding to conditions where previous work[14] has suggested close to 100% transmission through the funnel region for the analyte ions. Therefore, the overall transmission efficiencies of 70−80%, based on measurements of the total ion current (e.g., Figure 5), underestimate the actual transmission efficiencies for the analyte ions due to large charged clusters at high mass per charge and low mass per charge species contributing to the total measured current after the heated capillary.

The above optimization of the instrument parameters resulted in an increase in the total ion current to 765 pA for a 4×10^{-5} M horse myoglobin solution as measured at the rear trapping plate of the FTICR cell. When recorded, the mass spectrum of each individual charge state displayed only one peak (i.e. all isotopic species in the envelope were phase locked). Dilution of the sample reduced the total ion current delivered to the FTICR cell. Shown in Figure 7 is a mass spectrum obtained for a 4×10^{-7} M horse myoglobin solution which produced a total ion current of about 240 pA at the FTICR cell. The ion injection time was 0.2 s. The higher intensity charge state, $[M + 18H]^{18+}$, is phase-locked, while the lower intensity peaks, e.g. $[M + 20H]^{20+}$, reveal resolved isotopic patterns. Exciting ions to larger radii prevented phase locking of the isotopic peaks for the $[M + 18H]^{18+}$ charge state. This result is consistent with earlier predictions[21] that peak coalescence is a function of the ion population, mass per charge, and the cyclotron radius. Similarly, a larger trap and stronger magnetic field would be advantageous for preventing or minimizing phase-locking effects.

The dependence of the total ion current in the FTICR trap on the sample concentration is presented in Figure 8 for horse cytochrome *c* and horse myoglobin. The theoretical calculations shown are based upon the assumption of 100% ionization efficiency

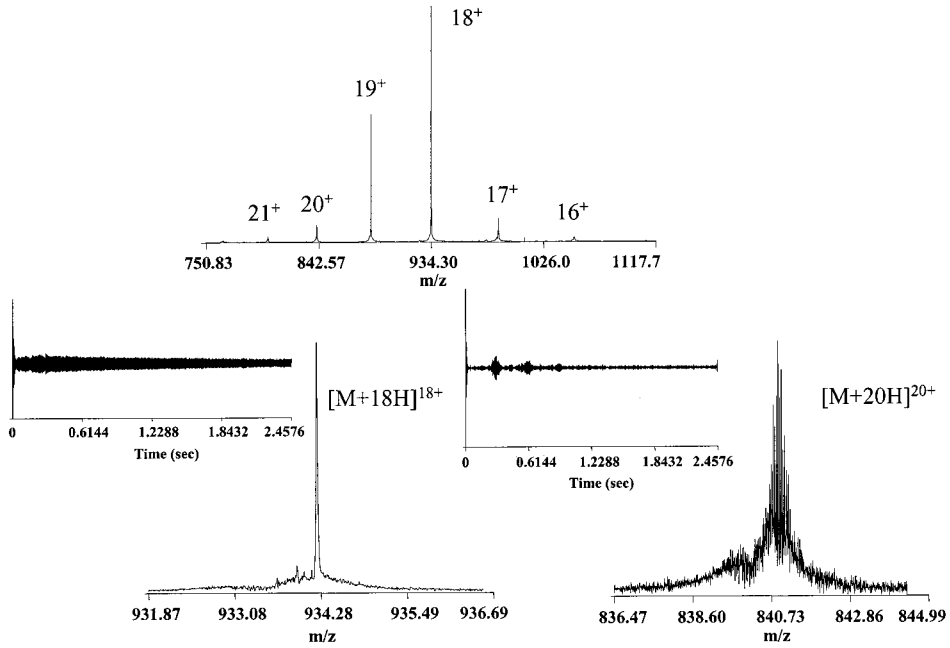

Figure 7. Mass spectrum for 4×10^{-7} M horse myoglobin. The insets show transients and magnitude spectra of $[M + 18H]^{18+}$ and $[M + 20H]^{20+}$ ions.

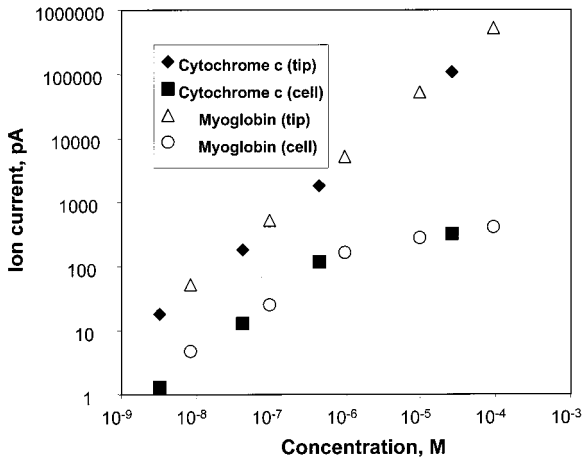

Figure 8. Total ion currents for horse cytochrome *c* and horse myoglobin in the FTICR cell as functions of sample concentration. Calculated values are based on eq 8.

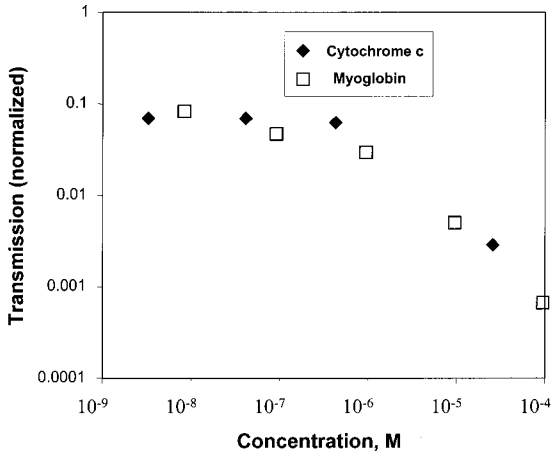

Figure 9. Transmission efficiency for horse cytochrome *c* and horse myoglobin ions as functions of sample concentration.

and 100% ion transmission and are derived from the relationship

$$\mathrm{TIC} = C[\mathrm{mol/L}]\mathit{Flow\_rate}[\mathrm{L/s}]t[\mathrm{s}]N_A q \qquad (8)$$

where TIC is the total analyte ion current injected into the FTICR mass spectrometer, C is the sample concentration in mol/L, *Flow_rate* is the syringe flow rate in L/s, t is the duration of a trapping event in s, and q is the average charge state of a protein. As seen in Figure 8, at sample concentrations below 10^{-6} M, the slopes of the theoretical (total analyte ion current at the tip predicted by eq 8) and experimental dependencies are similar, suggesting constant ionization efficiencies are achieved. Figure 9 shows transmission efficiency as a function of the sample concentration (each point represents a ratio of the experimental ion current to the theoretical prediction). Encouragingly, for sample concentrations below 10^{-6} M, the overall transmission efficiency of the instrument is virtually concentration-independent, corresponding to an overall transmission efficiency of 7−10%. As transmission of each element of the mass spectrometer was measured on the basis of a ratio of the output to the input ion currents of that particular element, 7% overall transmission efficiency implies that about 60% of the analyte ions dissolved in a diluted water/methanol/acetic acid solution reach the ion funnel. In other words, the overall efficiency of ionization, the efficiency of ion transport from the ESI emitter to the heated capillary inlet, and the transmission efficiency through the 0.75-mm-i.d. heated capillary are about 60%. Therefore, the efficiency of ionization approaches unity at a flow rate of 200 nL/min and at a sample concentration less than 10^{-6} M, i.e., for diluted samples electrosprayed at flow rates of a few hundred nanoliters per minute, microspray can provide an efficiency of ionization close to that of nanospray.

The probability of trapping ions in the FTICR cell as a result of ion−neutral collisions, P_{trap}, can be estimated on the basis of a hard-sphere collision model. The potentials applied to the front and rear trapping plates of the FTICR cell are adjusted to correspond to the kinetic energies of slowest and fastest ions entering the cell, and in order to be trapped in the cell an ion should be thermalized in collisions with a target gas. The details of estimation are given in Appendix A.

$$P_{\mathrm{trap}} = 2l_{\mathrm{trap}}\sigma_0 n_0 \frac{p_{\mathrm{cell}}}{p_{\mathrm{atm}}} \frac{m_{\mathrm{neutr}}}{m_{\mathrm{ion}} + m_{\mathrm{neutr}}} K \qquad (9)$$

$$K = \sqrt{\frac{U_{\mathrm{front}}}{\Delta U}}\log^{-1}\left(\frac{U_{\mathrm{front}}}{\Delta U} + \sqrt{\frac{U_{\mathrm{front}}}{\Delta U} + 1}\right) + \left(1 + \frac{U_{\mathrm{front}}}{\Delta U}\right)\frac{2}{\pi} \qquad (10)$$

Here, σ_0 is the gas-kinetic cross section of a molecular ion, n_0 is the Loschmidt's number, p_{cell} is the pressure in the FTICR cell during target gas injection, p_{atm} is the atmospheric pressure, l_{trap} is the cell length, m_{neutr} is the mass of a target gas (nitrogen), m_{ion} is the mass of the analyte ion, U_{front} is the potentials applied to the front trapping plate and ΔU is the kinetic energy spread per elementary charge. For the most abundant charge state, $[M + 15H]^{15+}$, in the mass spectrum of cytochrome *c*, σ_0 is about 2000×10^{-16} cm^2.[22] At p_{cell} of 3×10^{-6} Torr, l_{trap} of 8 cm, U_{front} of 6 V, and ΔU of 3 V, eq 9 gives a probability of trapping, P_{trap}, of about 3×10^{-3}. Substituting the estimated probability of ion trapping ($\sim 3 \times 10^{-3}$) and the overall transmission efficiency ($\sim 7 \times 10^{-2}$) into eq 4 results in a theoretical detection limit of about 50 zmol using the $[M + 15H]^{15+}$ species of cytochrome *c*.

Figure 10 shows the mass spectra from horse cytochrome *c* $[M + 15H]^{15+}$ and horse myoglobin $[M + 17H]^{17+}$ ions electrosprayed from solution at a concentration of 0.4 nM. Both spectra were obtained with a 0.2-s trapping event and a flow rate of 100 nL/min. The total amount of sample consumed for each protein was 135 zmol, exhibiting a signal-to-noise ratio of about 10:1. On the basis of sample consumption, we determined the detection limit to be about 30 zmol for both proteins (3×10^{-20} mole, or ~18 000 molecules) which is consistent with the above estimate.

Further improvement of the detection limit will require an increase in the FTICR trapping efficiency. According to eq 9, trapping efficiency is directly proportional to the pressure in the cell during a trapping event. Raising pressure above 10^{-5} Torr in the FTICR cell is constrained by the pumping speed of the

(21) Mitchell, D. W.; Smith, R. D. *Phys. Rev. E* **1995**, *52*, 4366−4386.

(22) Chen, Y.; Collings, B. A.; Douglas, D. J. *J. Am. Soc. Mass Spectrom.* **1997**, 681−687.

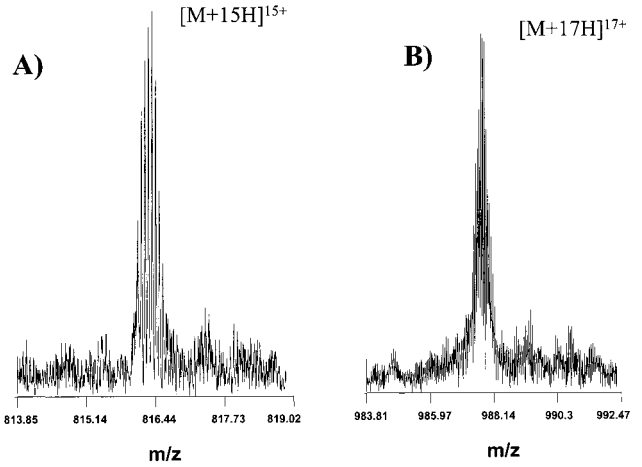

Figure 10. Portions of mass spectra showing $[M + 15H]^{15+}$ ions of horse cytochrome *c* (A) and $[M + 17]^{17+}$ ions of horse myoglobin (B). Sample concentrations were 0.4 nM. Total consumed for each protein was 135 *zmol* (∼ -81 300 molecules).

cryopanel pumping arrangement used to evacuate the ultrahigh vacuum region. Higher pressures will also result in faster saturation of the cryopanel (i.e., the need for more frequent regeneration). External accumulation of ions in a higher pressure region trapping should be more effective since an elevated pressure is either not required (i.e., gated trapping[23]) or is needed only for a much shorter period. Such modifications are in progress and promise to increase sensitivity to the one zeptomole level and perhaps below.

CONCLUSIONS

Optimization of the performance for a 3.5 T FTICR mass spectrometer equipped with an electrospray source and the electrodynamic ion funnel in the intermediate pressure region of the source has resulted in significant improvement of the overall ion transmission and has greatly increased sensitivity. It has been shown that introduction and optimization of the ion funnel in the pressure region of about 1−5 Torr, improving the ion beam characteristics in the quadrupole-electrostatic ion guide interface as well as modification of the electrostatic ion guide decreased the detection limit of the instrument to ∼30 zmol for smaller proteins. Further improvement in the instrument sensitivity will require increasing the probability of ion trapping. As shown by modeling, ion trapping in the external accumulation interface at a pressure of about 10^{-3} Torr would result in a probability of trapping close to unity and would enable improvement of the detection limit to the sub-zmol range. If achieved, such a sensitivity would bring FTICR mass spectrometry with its powerful capabilities to the cutting edge of proteomic technology (e.g., characterization of many proteins from a single cell).

ACKNOWLEDGMENT

The authors are grateful to Drs. Aleksey Tolmachev, Christophe Masselon, Richard Harkewicz, David Prior, and Eugene Nikolaev for helpful discussions. The ESI-FTICR instrumentation design and construction was supported as part of the development of the Environmental Molecular Sciences Laboratory at Pacific Northwest National Laboratory (PNNL) by the office of Biological and Environmental Research, U. S. Department of Energy. The ion funnel implementation was supported by the NIH National Center for Research Resources under Grant RR12365. PNNL is a multiprogram national laboratory operated by Battelle Memorial Institute for the US Department of Energy under Contract DE-AC06-76RLO 1830.

APPENDIX A

We assume that the approximation of a quadrupole field is applicable to an 8-cm-i.d., 8-cm-long cylindrical cell. The potentials applied to the front, U_{front}, and rear, U_{rear}, trapping plates correspond to the slowest and fastest ions entering the cell, respectively. FTICR cell detection and excitation side plates are maintained at ground potential during trapping.

Let us consider the motion of an individual ion between the front trapping plate and the middle of the cell. The ion has an initial kinetic energy of $qe\Delta U$, where q is the ion charge, e is the elementary charge, ΔU is the kinetic energy spread of an ion beam per elementary charge. The ion velocity as a function of its coordinate along the z axis of the FTICR cell is given by

$$v(z) = \sqrt{\frac{2qe\left(\Delta U + U_{\text{front}}\frac{z^2}{d^2}\right)}{m_{\text{ion}}}} \qquad (11)$$

where m_{ion} is the ion mass and d is the half-length of the cell.

The ion reaches the middle of the cell after time T_1.

$$T_1 = \int_0^d \frac{dz}{v(z)} = \sqrt{\frac{m_{\text{ion}}d^2}{2qeU_{\text{front}}}}\log\left(\frac{U_{\text{front}}}{\Delta U} + \sqrt{\frac{U_{\text{front}}}{\Delta U} + 1}\right) \qquad (12)$$

As the ion spends different amounts of time in different regions of the cell, we introduce the probability to find the ion in the interval from z to $z + dz$, dP_1:

$$dP_1 = \frac{dt}{T_1} = \frac{dz}{v(z)T_1} \qquad (13)$$

The probability of ion−neutral collision, P_2, at distance z from the front trapping plate can be estimated as

$$P_2 = 1 - \exp\left(-zn_0\frac{p_{\text{cell}}}{p_{\text{atm}}}\sigma_0\right) \qquad (14)$$

where n_0 is Loschmidt's number, p_{cell} is the pressure in the cell, p_{atm} is the atmospheric pressure, σ_0 is the gas-kinetic cross section of the analyte ion. Due to relatively low pressure in the cell during pulsed gas injection (typically $\sim 10^{-6}$ Torr), the exponential term of eq 14 can be reduced to the first term of Taylor's expansion as follows:

$$P_2 = zn_0\frac{p_{\text{cell}}}{p_{\text{atm}}}\sigma_0 \qquad (15)$$

(23) Senko, M. W.; Hendrickson, C. L.; Emmett, M. R.; Shi, S. D.; Marshall, A. G. *J. Am. Soc. Mass Spectrom.* **1997**, *8*, 970−976.

On the basis of the energy and momentum conservation laws, the ion velocity after collision with a neutral molecule (hard-sphere model) is governed by

$$v_{\text{after}}(z) = v_{\text{before}}(z)\frac{m_{\text{ion}} - m_{\text{neutral}}}{m_{\text{ion}} + m_{\text{neutral}}} \tag{16}$$

where $v_{\text{before}}(z)$ and $v_{\text{after}}(z)$ are the ion velocities before and after collision, respectively.

The probability-weighed velocity change when the ion reaches the middle of the cell can be estimated as:

$$\Delta v_1 = \frac{\int_0^{P_1}(v_{\text{before}}(z) - v_{\text{after}}(z))P_2 dP_1}{\int_0^{P_1} dP_1} \tag{17}$$

Substituting eqs 13, 15, 16 into eq 17 and then integrating eq 17 within limits from 0 to d gives

$$\Delta v_1 = \frac{m_{\text{neutral}}}{m_{\text{ion}} + m_{\text{neutral}}} n_0 \frac{p_{\text{cell}}}{p_{\text{atm}}} \sigma_0 d^2 \frac{1}{T_1} \tag{18}$$

The kinetic energy loss, ΔE_1, experienced by an ion due to ion−neutral collisions is related to the above velocity change as

$$\Delta E_1 = \frac{m_{\text{ion}}}{2}(2v_{\text{before}}(0)\Delta v_1 - \Delta v_1{}^2) \tag{19}$$

$$v_{\text{before}}(0) = \sqrt{\frac{2qe\Delta U}{m_{\text{ion}}}} \tag{20}$$

Noting that Δv_1 is proportional to $m_{\text{neutral}}/m_{\text{ion}}$, we neglect the second term in eq 19. Substituting eqs 12, 18, 20 into eq 19 gives the relationship for the kinetic energy loss due to ion−neutral collisions when an ion reaches the middle of the cell

$$\Delta E_1 = qe\sqrt{\Delta U U_{\text{front}}}\frac{m_{\text{neutral}}}{m_{\text{ion}} + m_{\text{neutral}}} \times \log^{-1}\left(\frac{U_{\text{front}}}{\Delta U} + \sqrt{\frac{U_{\text{front}}}{\Delta U} + 1}\right) n_0 \frac{p_{\text{cell}}}{p_{\text{atm}}} \sigma_0 l_{\text{trap}} \tag{21}$$

l_{trap} is the cell length.

Similarly, the kinetic energy loss in the region between the middle of the cell and the rear trapping plate can be derived. The velocity of an ion in this region is governed by the following:

$$v(z) = \sqrt{\frac{2qe(\Delta U + U_{\text{front}})\left(1 - \frac{z^2}{d^2}\right)}{m_{\text{ion}}}} \tag{22}$$

The ion reaches the rear trapping plate after time T_2

$$T_2 = \int_0^d \frac{dz}{v(z)} = \sqrt{\frac{m_{\text{ion}} d^2}{2qe(U_{\text{front}} + \Delta U)}}\frac{\pi}{2} \tag{23}$$

Following the logic described in eqs 11−21, the kinetic energy loss in the region between the middle of the cell and the rear trapping plate is then given by the following:

$$\Delta E_2 = qe(\Delta U + U_{\text{front}})\frac{m_{\text{neutral}}}{m_{\text{ion}} + m_{\text{neutral}}} n_0 \frac{p_{\text{cell}}}{p_{\text{atm}}} \sigma_0 l_{\text{trap}} \frac{2}{\pi} \tag{24}$$

Kinetic energy loss experienced by an ion after one passage through the cell is governed by the following:

$$\Delta E = \Delta E_1 + \Delta E_2 = qe\Delta U \frac{m_{\text{neutral}}}{m_{\text{ion}} + m_{\text{neutral}}} n_0 \frac{p_{\text{cell}}}{p_{\text{atm}}} \sigma_0 l_{\text{trap}} K \tag{25}$$

$$K = \sqrt{\frac{U_{\text{front}}}{\Delta U}}\log^{-1}\left(\frac{U_{\text{front}}}{\Delta U} + \sqrt{\frac{U_{\text{front}}}{\Delta U} + 1}\right) + \left(1 + \frac{U_{\text{front}}}{\Delta U}\right)\frac{2}{\pi} \tag{26}$$

When an ion returns to the front trapping plate the above kinetic energy loss doubles. An ion will be trapped in the cell if its kinetic energy loss is equal to the ion's initial kinetic energy. Therefore, the probability of trapping an ion in the FTICR cell can be estimated as:

$$P_{\text{trap}} = 1 - \exp\left(-\frac{\Delta E}{qe\Delta U}\right) \cong \frac{\Delta E}{qe\Delta U} = \frac{2m_{\text{neutral}}}{m_{\text{ion}} + m_{\text{neutral}}} n_0 \frac{p_{\text{cell}}}{p_{\text{atm}}} \sigma_0 l_{\text{trap}} K \tag{27}$$

Received for review November 24, 1999. Accepted February 24, 2000.

AC991360B